ELSEVIER

Journal of Organometallic Chemistry 529 (1997) 409–422

Journal of Organometallic Chemistry

Molybdenum carbonyl complexes of di- and triphosphines: hydrophosphination reactions of $(HC{\equiv}CCH_2PPh_2)Mo(CO)_5$

Kalyani Maitra, Vincent J. Catalano, John H. Nelson *

Department of Chemistry, University of Nevada, Reno, NV 89557-0020, USA

Received 24 April 1996; revised 17 June 1996

Abstract

The base catalyzed hydrophosphination reactions of $(HC{\equiv}CCH_2PPh_2)Mo(CO)_5$ with Ph_2PH and $(Ph_2PH)Mo(CO)_5$ give several different products as a function of reaction conditions. These products were characterized by elemental analyses, physical properties, ^1H, $^{13}C\{^1H\}$, and $^{31}P\{^1H\}$ NMR spectroscopy, infrared spectroscopy, and in most cases by X-ray crystallography.

Keywords: Diphosphine; Nuclear magnetic resonance; Molybdenum; Hydrophosphination

1. Introduction

The base catalyzed addition of secondary phosphines to activated carbon–carbon multiple bonds (hydrophosphination) is an efficient, established pathway for preparing chelating tertiary diphosphines which are very important in coordination and organometallic chemistry and in associated areas of catalysis [1]. A variety of examples is known where the phosphine is prepared separately and then complexed to an appropriate transition metal [2,3]. An alternative approach involves the syntheses of the ligands in complexed form using reactions of phosphines which are already coordinated to the metal [4].

Secondary phosphines are known to undergo *trans*-addition to free phosphino alkynes [5] and *cis*-addition to coordinated phosphino alkynes [6]. Coordination of a phosphino alkyne to a transition metal greatly modifies the reactivity of the alkyne moiety, making it susceptible to reactions such as hydration [7], hydrogen halide addition [8], and acetylene coupling [9]. Analogous activation towards hydrophosphination by secondary phosphines has also been reported [6]. Such addition reactions may provide an efficient route for the syntheses of unsymmetrical, rigid, chelating diphosphine ligands, which have potential applications in the rich prolific area of asymmetric catalysis [10]. Previously, as part of extensive studies into reactions of this type, we reported that reaction of the secondary phosphole complex $(HDBP)Mo(CO)_5$ with the phosphino alkyne complex $(HC{\equiv}CCH_2DBP)Mo(CO)_5$ gives the chelate complex *cis*-$[DBPCH{=}C(CH_3)DBP]Mo(CO)_4$ (reaction (1)) [11].

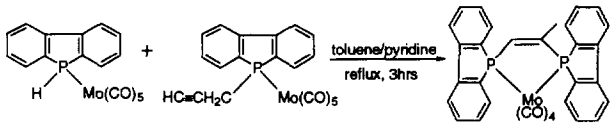

(1)

We now report that, under more forcing conditions, reactions of the phosphino alkyne complex **2c** with free diphenyl phosphine (Ph_2PH) in the presence of a catalytic amount of potassium *t*-butoxide produces the chelating diphosphine complex **6** in high yield. Similarly, the reactions of **2a** with the secondary phosphine complex $(Ph_2PH)Mo(CO)_5$ (**1**), performed under different reaction conditions, produce either complexes **4** and **5** or complex **5** along with other products. The thermally induced elimination of $Mo(CO)_6$ from complex **4**, under forcing conditions, produces a mixture of complex **5** and its isomer **6**. We were also able to isolate the tricarbonyl triphosphine complex **7** and the bridged phosphide complex **8** as by-products under different

* Corresponding author.

PII S0022-328X(96)06599-0

reaction conditions. The structures of complexes **3–8** were deduced by ^{1}H, $^{31}P\{^{1}H\}$ and $^{13}C\{^{1}H\}$ NMR and IR spectroscopies. In most cases the structures were confirmed by single crystal X-ray diffraction studies. The structure of complex **9** containing the pendant free phosphine arm was established only from $^{31}P\{^{1}H\}$ NMR spectroscopy and X-ray structure analysis.

2. Results and discussion

Recently, we reported a convenient route to phosphine complexes of the type $(RPPh_2)Mo(CO)_5$, where R is a variety of alkyl groups or hydrogen [12]. We also found that the phosphino alkyne complex $(HC{\equiv}CCH_2PPh_2)Mo(CO)_5$ (**2a**) isomerizes in refluxing tetrahydrofuran (THF) in the presence of base to produce a mixture of all three isomers **2a**, **2b** and **2c** (propargyl, allenyl and propynyl) respectively in solution, which could be separated by column chromatography [12].

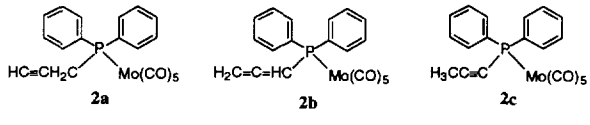

Treatment of an equimolar mixture of $(HPPh_2)Mo(CO)_5$ (**1**) and $(HC{\equiv}CCH_2PPh_2)Mo(CO)_5$ (**2a**) in the presence of potassium *t*-butoxide in refluxing THF gave complexes **3**, **4** and **5** in the crude mixture as indicated by $^{31}P\{^{1}H\}$ NMR spectroscopy (Scheme 1). Purification by column chromatography, followed by recrystallization from a 1:1 mixture of dichloromethane and methanol, yielded 14.7%, 31.2% and 40% of pale yellow to almost colorless crystals of **3**, **4** and **5** respectively.

Under more forcing conditions, in refluxing diglyme, the crude reaction mixture contained complexes **3**, **5**, **7** and **8**, as indicated by $^{31}P\{^{1}H\}$ NMR spectroscopy (Scheme 2). Separation of the complexes by column chromatography, followed by recrystallization from a 1:1 mixture of dichloromethane and methanol, yielded

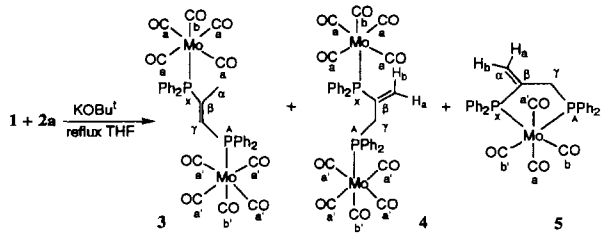

Scheme 1.

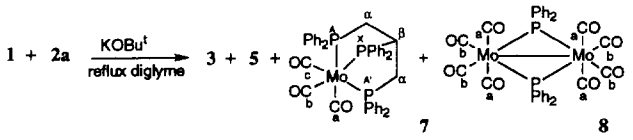

Scheme 2.

27%, 46%, 7.6% and 11.2% of complexes **3**, **5**, **7** and **8** respectively. The crystals of complex **7** were flaky and colorless, while those of complex **8** were deep red in color. Our initial attempts at conducting this hydrophosphination reaction with **1** and **2a** in the presence of pyridine in refluxing toluene, while maintaining the same reaction environment as mentioned in reaction (1) [11], did not give the expected products but instead resulted in isomerization of **2a** to **2c** [12]. Previously, we concluded from structural and spectroscopic data [11,12] that the π-acceptor ability of the phosphole ligands RDBP is greater than that of the $RPPh_2$ analogs, causing the molybdenum complexes of the latter to be less reactive towards hydrophosphination. Hence, the presence of a stronger base such as potassium *t*-butoxide was necessary to initiate the addition reactions.

Addition of the P–H bond in complex **1**, across the acetylenic moiety of complex **2a** in refluxing THF (Scheme 1), occurs exclusively in a Markovnikov sense to give the *geminal* regio-isomer **4**, as indicated by the presence of the two *geminal* vinyl proton (H_a, H_b) resonances in the ^{1}H NMR spectrum. Base catalyzed migration of the double bond in complex **4** by a [1, 3] hydrogen shift gives the thermodynamically more stable dimolybdenum species **3**, with the phosphine moieties oriented *trans* to each other. As stated earlier, the allenyl isomer **2b** and the propynyl isomer **2c** can be generated in the reaction mixture by similar [1, 3] hydrogen shift rearrangements of **2a**. The possibility that complex **3** may form from the addition of **1** to **2c** was dismissed, since the recovered starting materials from all the addition reactions of **1** and **2a** conducted in THF or diglyme consisted of minor amounts of unreacted **1**, diphenyl phosphine oxide and mainly the rearranged isomer **2c**. Moreover, direct reaction of complex **1** with **2c** in refluxing diglyme in the presence of base gave complex **8** and some decomposed products of **1** along with the total recovery of **2c**. The absence of the allenyl isomer **2b** as a recovered product from any of the reactions inferred that this form of the rearranged isomer, even if present in solution, undergoes the P–H addition in a Markovnikov's sense with complex **1**, across its terminal vinyl or internal vinyl functions, to produce complexes **3** and **4** respectively. We thus conclude that **2c** is less reactive than its isomers **2a** and **2b**, and therefore the presence of a stronger base is necessary to initiate its addition reactions.

The $^{31}P\{^{1}H\}$ NMR spectra of complexes **3** and **4** each show the presence of a pair of inequivalent ^{31}P nuclei in

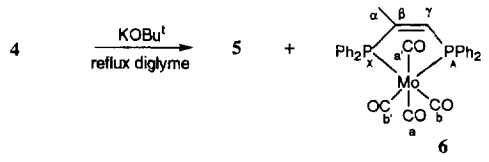

Scheme 3.

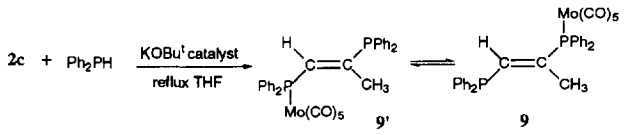

Scheme 5.

each complex with $^{3}J_{PP}$ values of 26.91 and 15.27 Hz respectively. The *trans* geometry of the two phosphorus nuclei across the double bond in complex **3** enhances the coupling between the two phosphorus atoms through conjugation, giving a higher splitting value than observed for its isomer **4**. Complex **4** also underwent thermally induced $Mo(CO)_6$ elimination to produce the exomethylene chelate complex **5**. This conclusion was verified as, under more forcing conditions, refluxing complex **4** in diglyme in the presence of KO^{t}Bu produced complexes **5** and **6** as the only products in 51.6% and 33.6% yield respectively (Scheme 3). The absence of complex **3** from the product mixture indicates that the most likely mechanism of the reaction therefore appears to be first chelation, to give **5**, followed by base promoted [1, 3] hydrogen migration to give the thermodynamically more stable isomeric product **6** [13–15]. This was further confirmed since pure complex **5** underwent quantitative KO^{t}Bu catalyzed isomerization in refluxing diglyme to form complex **6**. For complexes **5** and **6**, $^{31}P\{^1H\}$ NMR spectroscopy shows the presence of two inequivalent phosphorus nuclei in each case with $^{3}J_{PP}$ values of 7.48 and 6.33 Hz respectively. Interestingly, for these chelate complexes the additional coupling pathway for the two phosphorus atoms through the metal backbone decreases the coupling constant value as compared with the values observed for complexes **3** and **4** [16].

The hydrophosphination reaction of **1** with **2a**, conducted in diglyme, yielded complex **5** as one of the major products and, as expected, the intermediate complex **4** was absent (Scheme 2) from the product mixture. The high refluxing temperature and the presence of the strong base caused other side reactions to occur, leading to the formation of complexes **7** and **8**. Most likely, the addition of one molecule of complex **1** across the double bond of complex **5** in an anti-Markovnikov's sense followed by chelation yielded complex **7**, having the facial configuration. The anti-Markovnikov addition rather than Markovnikov addition may be a result of steric effects. The synthesis of complex **7** has been reported earlier under somewhat similar reaction conditions [2]. However, the intermediate addition product, containing the pendant metal coordinated phosphine,

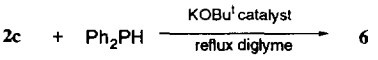

Scheme 4.

was not detected in the product mixture probably due to its complete conversion into complex **7** under the forcing reaction conditions. The $^{31}P\{^1H\}$ NMR spectrum for complex **7** shows the presence of two types of inequivalent phosphorus atoms with an integral ratio of 2:1 (δ = 40.96 and 82.92 ppm, $^{2}J_{PP}$ = 1.52 Hz). The bridged complex **8**, obtained as a minor product in this reaction, is formed from the condensation of two equivalents of complex **1** in the presence of base with the elimination of two CO units. Complex **8** has been reported earlier [17]. It was prepared under similar conditions as used purposefully for preparing complexes of this type. The $^{31}P\{^1H\}$ NMR spectrum of **8** shows the presence of only one kind of phosphorus nucleus (δ = 231.71 ppm), and its $^{13}C\{^1H\}$ NMR spectrum (see Section 3) is also

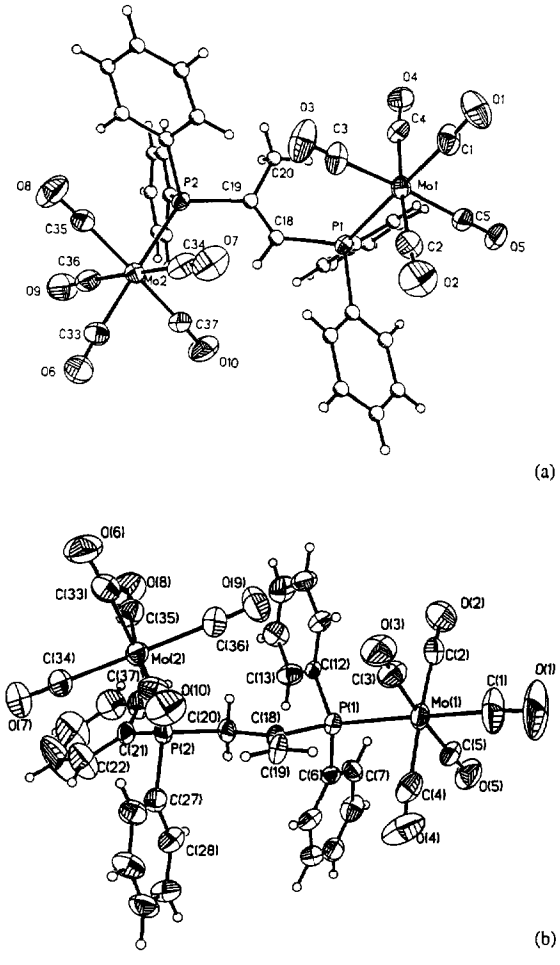

Fig. 1. Structural drawings of (a) **3** and (b) **4** showing the atom numbering scheme (40% probability ellipsoids). Hydrogen atoms have an arbitrary radius of 0.1 Å.

consistent with its structure. The resonance for the equatorial carbonyl carbons situated *trans* to the phosphorus atoms exhibits a second order $A[X]_2$ splitting pattern in the $^{13}C\{^1H\}$ NMR spectrum. In contrast, the axial carbonyl carbon resonance is a first order triplet with a $^2J_{PC}$ value of 5.22 Hz.

In order to optimize the yield of complex **6** and also study the reaction of a coordinated phosphino alkyne with a simple secondary phosphine, complex **2c** was reacted in refluxing diglyme with Ph_2PH; a stronger nucleophile than the metal coordinated secondary phosphine. This reaction produced complex **6** as the only isolated product in 73% yield (Scheme 4). The same reaction performed in refluxing THF yielded complexes **3** and **6** in minor quantities along with a range of other products that could not be separated by column chromatography. Crystallization from a 1:1 mixture of CH_2Cl_2 and MeOH gave pale yellow crystals that consisted of a mixture of compounds as shown by $^{31}P\{^1H\}$ NMR spectroscopy. X-ray crystallography of a

Table 1
Selected bond lengths (Å) and angles (°) for **3**

Bond lengths			
Mo(1)–C(4)	1.999(12)	Mo(1)–C(1)	2.002(13)
Mo(1)–C(5)	2.006(12)	Mo(1)–C(3)	2.034(12)
Mo(1)–C(2)	2.039(12)	Mo(1)–P(1)	2.541(3)
Mo(2)–C(37)	1.999(13)	Mo(2)–C(33)	2.009(13)
Mo(2)–C(34)	2.017(13)	Mo(2)–C(35)	2.027(13)
Mo(2)–C(36)	2.036(14)	Mo(2)–P(2)	2.516(3)
P(1)–C(18)	1.822(9)	P(1)–C(6)	1.837(10)
P(1)–C(12)	1.841(10)	P(2)–C(27)	1.834(9)
P(2)–C(21)	1.854(9)	P(2)–C(19)	1.868(9)
O(1)–C(1)	1.116(13)	O(2)–C(2)	1.130(13)
O(3)–C(3)	1.120(12)	O(4)–C(4)	1.137(13)
O(5)–C(5)	1.150(12)	O(6)–C(33)	1.125(14)
O(7)–C(34)	1.127(13)	O(8)–C(35)	1.148(13)
O(9)–C(36)	1.130(14)	O(10)–C(37)	1.130(13)
C(18)–C(19)	1.319(11)	C(19)–C(20)	1.519(14)
Bond angles			
C(4)–Mo(1)–C(1)	86.3(5)	C(4)–Mo(1)–C(5)	91.4(5)
C(1)–Mo(1)–C(5)	91.7(5)	C(4)–Mo(1)–C(3)	92.5(5)
C(1)–Mo(1)–C(3)	87.6(5)	C(5)–Mo(1)–C(3)	175.9(5)
C(4)–Mo(1)–C(2)	174.6(5)	C(1)–Mo(1)–C(2)	88.4(5)
C(5)–Mo(1)–C(2)	87.8(5)	C(3)–Mo(1)–C(2)	88.1(5)
C(4)–Mo(1)–P(1)	93.0(3)	C(1)–Mo(1)–P(1)	179.2(4)
C(5)–Mo(1)–P(1)	88.6(3)	C(3)–Mo(1)–P(1)	92.1(3)
C(2)–Mo(1)–P(1)	92.3(3)	C(37)–Mo(2)–C(33)	88.9(5)
C(37)–Mo(2)–C(34)	93.4(4)	C(33)–Mo(2)–C(34)	88.6(5)
C(37)–Mo(2)–C(35)	176.4(5)	C(33)–Mo(2)–C(35)	91.7(5)
C(34)–Mo(2)–C(35)	90.2(5)	C(37)–Mo(2)–C(36)	88.5(5)
C(33)–Mo(2)–C(36)	89.5(6)	C(34)–Mo(2)–C(36)	177.3(6)
C(35)–Mo(2)–C(36)	87.9(5)	C(37)–Mo(2)–P(2)	90.8(4)
C(33)–Mo(2)–P(2)	177.0(4)	C(34)–Mo(2)–P(2)	88.4(4)
C(35)–Mo(2)–P(2)	88.8(3)	C(36)–Mo(2)–P(2)	93.4(4)
C(18)–P(1)–C(6)	102.9(4)	C(18)–P(1)–C(12)	102.0(4)
C(6)–P(1)–C(12)	103.0(4)	C(18)–P(1)–Mo(1)	117.8(3)
C(6)–P(1)–Mo(1)	118.8(3)	C(12)–P(1)–Mo(1)	110.1(3)
C(27)–P(2)–C(21)	105.0(4)	C(27)–P(2)–C(19)	101.3(4)
C(21)–P(2)–C(19)	99.9(4)	C(27)–P(2)–Mo(2)	112.3(3)
C(21)–P(2)–Mo(2)	117.1(3)	C(19)–P(2)–Mo(2)	119.0(3)
O(1)–C(1)–Mo(1)	177.6(12)	O(2)–C(2)–Mo(1)	174.7(12)
O(3)–C(3)–Mo(1)	176.0(10)	O(4)–C(4)–Mo(1)	174.2(11)
O(5)–C(5)–Mo(1)	177.9(11)	C(11)–C(6)–C(7)	118.6(10)
C(19)–C(18)–P(1)	126.5(8)	C(18)–C(19)–C(20)	124.5(9)
C(18)–C(19)–P(2)	119.3(8)	C(20)–C(19)–P(2)	116.1(6)
O(6)–C(33)–Mo(2)	177.8(12)	O(7)–C(34)–Mo(2)	176.7(12)
O(8)–C(35)–Mo(2)	176.3(11)	O(9)–C(36)–Mo(2)	176.8(11)
O(10)–C(37)–Mo(2)	177.6(11)		

single crystal taken from this mixture showed the complex to have the unexpected structure **9** (as shown in Fig. 4). A suggested mechanistic pathway for the formation of complex **9** is shown in Scheme 5.

The presence of the methyl group on the metal coordinated end of the diphosphine, as in **9**, suggests that the hydrophosphination reaction of **2c** and Ph_2PH first produces the intermediate product **9′** (by analogy with the previously discussed reactions), which then exchanges the bound and dangling ends of the ligand to finally produce **9** in the product mixture. Examples of such exchange reactions between the bound and dangling ends of diphosphine ligands have previously been reported by other research groups [18].

2.1. Single crystal X-ray analysis of complexes 3, 4, 5, 6, 8 and 9

Crystals of all six compounds (**3–6** and **8–9**) suitable for X-ray analysis were grown by slow diffusion of methanol into dichloromethane solutions. Each structure consists of isolated molecules with no unusual intermolecular contacts. The molecular structures of **3** and **4** are shown in Fig. 1, and selected bond distances and angles are listed in Tables 1 and 2 respectively. Complexes **3** and **4** each contain two metal pentacarbonyl units bound to the two phosphorus atoms of the isomeric bidentate ligands $Ph_2PCH{=}C(CH_3)PPh_2$ and $Ph_2PCH_2C(=CH_2)PPh_2$ respectively. In each case the

Table 2
Selected bond lengths (Å) and angles (°) for **4**

Bond lengths			
Mo(1)–C(1)	1.972(14)	Mo(1)–C(4)	2.027(14)
Mo(1)–C(2)	2.034(14)	Mo(1)–C(5)	2.029(12)
Mo(1)–C(3)	2.047(12)	Mo(1)–P(1)	2.529(3)
Mo(2)–C(33)	1.962(13)	Mo(2)–C(35)	2.010(12)
Mo(2)–C(37)	2.028(12)	Mo(2)–C(34)	2.040(13)
Mo(2)–C(36)	2.059(13)	Mo(2)–P(2)	2.533(3)
P(1)–C(6)	1.815(9)	P(1)–C(12)	1.820(8)
P(1)–C(18)	1.853(9)	P(2)–C(27)	1.825(10)
P(2)–C(20)	1.826(8)	P(2)–C(21)	1.830(9)
O(1)–C(1)	1.117(13)	O(2)–C(2)	1.160(14)
O(3)–C(3)	1.129(12)	O(4)–C(4)	1.131(13)
O(5)–C(5)	1.130(11)	O(6)–C(33)	1.176(12)
O(7)–C(34)	1.125(12)	O(8)–C(35)	1.134(11)
O(9)–C(36)	1.113(12)	O(10)–C(37)	1.126(11)
C(18)–C(19)	1.305(11)	C(18)–C(20)	1.502(11)
Bond angles			
C(1)–Mo(1)–C(4)	90.8(6)	C(1)–Mo(1)–C(2)	88.3(6)
C(4)–Mo(1)–C(2)	176.2(5)	C(1)–Mo(1)–C(5)	87.1(5)
C(4)–Mo(1)–C(5)	89.1(4)	C(2)–Mo(1)–C(5)	87.2(5)
C(1)–Mo(1)–C(3)	89.4(5)	C(4)–Mo(1)–C(3)	91.6(5)
C(2)–Mo(1)–C(3)	92.1(5)	C(5)–Mo(1)–C(3)	176.4(5)
C(1)–Mo(1)–P(1)	178.6(5)	C(4)–Mo(1)–P(1)	89.5(4)
C(2)–Mo(1)–P(1)	91.3(4)	C(5)–Mo(1)–P(1)	91.5(3)
C(3)–Mo(1)–P(1)	92.0(3)	C(33)–Mo(2)–C(35)	88.3(5)
C(33)–Mo(2)–C(37)	88.5(4)	C(35)–Mo(2)–C(37)	171.6(5)
C(33)–Mo(2)–C(34)	87.5(5)	C(35)–Mo(2)–C(34)	92.9(5)
C(37)–Mo(2)–C(34)	94.8(5)	C(33)–Mo(2)–C(36)	91.9(5)
C(35)–Mo(2)–C(36)	86.2(5)	C(37)–Mo(2)–C(36)	86.1(5)
C(34)–Mo(2)–C(36)	178.9(5)	C(33)–Mo(2)–P(2)	172.5(4)
C(35)–Mo(2)–P(2)	88.2(3)	C(37)–Mo(2)–P(2)	95.9(3)
C(34)–Mo(2)–P(2)	86.0(3)	C(36)–Mo(2)–P(2)	94.5(3)
C(6)–P(1)–C(12)	105.5(4)	C(6)–P(1)–C(18)	102.0(4)
C(12)–P(1)–C(18)	101.3(4)	C(6)–P(1)–Mo(1)	111.5(3)
C(12)–P(1)–Mo(1)	116.2(3)	C(18)–P(1)–Mo(1)	118.6(3)
C(20)–P(2)–C(21)	99.0(4)	C(20)–P(2)–Mo(2)	116.9(3)
O(1)–C(1)–Mo(1)	177(2)	O(2)–C(2)–Mo(1)	176.3(14)
O(3)–C(3)–Mo(1)	176.3(10)	O(4)–C(4)–Mo(1)	176.9(11)
O(5)–C(5)–Mo(1)	176.4(10)	C(19)–C(18)–C(20)	124.8(8)
C(19)–C(18)–P(1)	121.4(7)	C(20)–C(18)–P(1)	113.8(6)
C(18)–C(20)–P(2)	120.1(6)	O(6)–C(33)–Mo(2)	175.4(11)
O(7)–C(34)–Mo(2)	178.0(12)	O(8)–C(35)–Mo(2)	175.7(11)
O(9)–C(36)–Mo(2)	176.8(11)	O(10)–C(37)–Mo(2)	175.8(10)

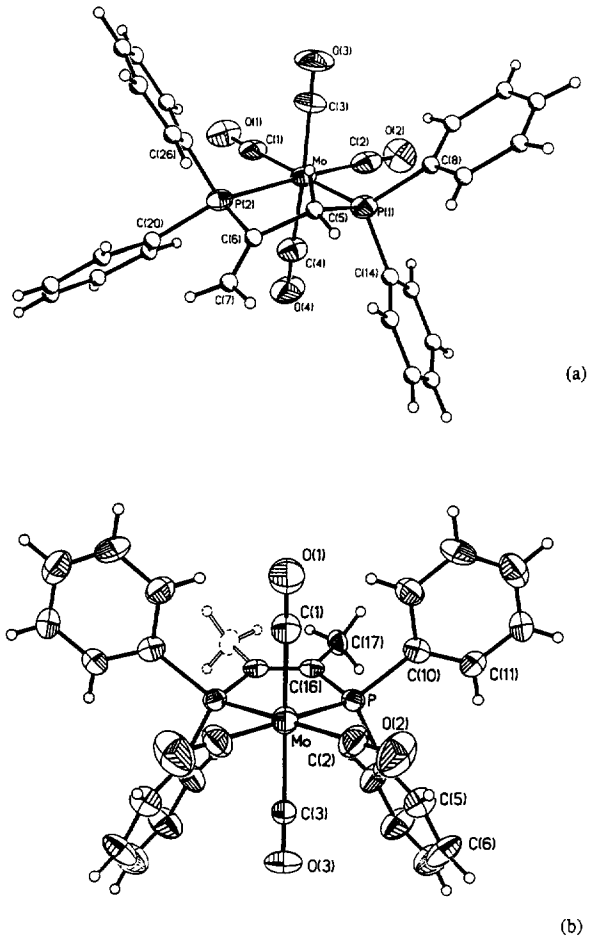

Fig. 2. Structural drawings of (a) **5** and (b) **6** showing the atom numbering scheme (40% probability ellipsoids). Hydrogen atoms have an arbitrary radius of 0.1 Å.

coordination geometries around both metal centers in **3** and **4** are distorted octahedrons formed from the ligation of five terminal CO groups and the phosphorus atom of the phosphine moiety. The Mo–P bond lengths for these complexes lie within the range 2.541–2.516 Å, which is in agreement with other reported values [3]. For complex **3**, containing the *trans* diphosphino ethene moiety, the C–O (1.125(14) Å) bond *trans* to P2 is essentially the same length as the C–O (1.116(13) Å) bond *trans* to P1. These CO bond lengths are essentially the same as the average value for the other eight CO bond lengths (1.134(14) Å). In contrast, for complex **4** the C–O (1.117(13) Å) bond *trans* to P1 has a shorter bond length than the C–O (1.176(12) Å) bond *trans* to P2. Here, the presence of the vinyl ($=CH_2$) group on C18 *geminal* to P1 makes the latter a poorer σ-donor as compared with P2 present at the other end of the ligand, and therefore the C–O bond *trans* to P1 is shorter. However, in complex **3** the direct linkage of P1 and P2 (*trans* to each other) to the ethylene function at C18 and C19 respectively decreases the σ-donor ability of both phosphorus atoms considerably, and hence the C–O bond distances of the *trans* and *cis* carbonyls are comparable with each other. Interestingly, for complex **4** the C–O bond *trans* to P2 has a greater bond length than the four *cis* C–O bonds due to the increased donor ability of P2 arising from its linkage to the alkyl unit, C20. For complex **3**, the distances C18–C19 and C19–C20 are 1.319(11) and 1.519(14) Å respectively, which confirms the presence of a double bond in the former case and a single bond in the latter case. Moreover, the interbond angles C20–C19–C18 and C19–C18–P1 are 124.5(9)° and 126.5(8)° respectively, which signifies that C19 and C18 are essentially sp^2 hybridized. Similarly, for complex **4** the carbon–carbon bond distances of 1.305(11) Å for C18–C19 and 1.502(11) Å for C18–C20 confirm the presence of double and single bonds respectively.

The molecular structures of the chelate diphosphine complexes **5** and **6** are shown in Fig. 2. Selected bond distances and angles are listed in Tables 3 and 4 respectively. The crystal structure of complex **6** shows a packing disorder within the crystal lattice. In each unit cell, half the molecules pack with methyl groups on one side, while the rest are flipped by 180° and, therefore, the unit cell as such appears to have a pseudo-mirror plane. Complexes **5** and **6** both have a distorted octahedral geometry at the metal center, where the equatorial plane is formed by the two P atoms and the two CO units *trans* to it. This distortion may be attributed largely to the formation of the five-membered ring and also to the differences between the Mo–P and Mo–CO bond lengths. In complex **5** the Mo–P2 distance (2.764(4) Å) is greater than the Mo–P1 distance (2.474(4) Å), as expected since the vinyl phosphine (P2)

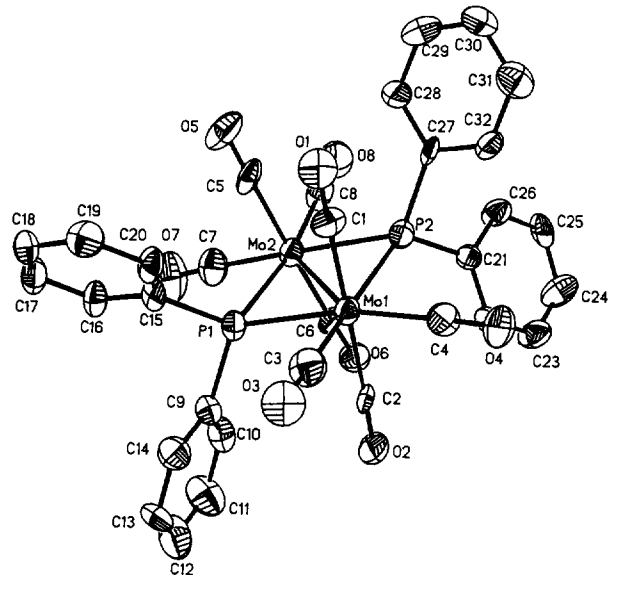

Fig. 3. Structural drawing of **8** showing the atom numbering scheme (40% probability ellipsoids). Hydrogen atoms have been omitted for clarity.

Table 3
Selected bond lengths (Å) and angles (°) for **5**

Bond lengths			
Mo–P(2)	2.746(4)	Mo–P(1)	2.474(4)
Mo–C(1)	1.959(15)	Mo–C(2)	2.173(17)
Mo–C(3)	1.883(14)	Mo–C(4)	1.898(14)
P(2)–C(6)	1.840(15)	P(2)–C(20)	1.890(13)
P(2)–C(26)	1.706(13)	P(1)–C(5)	1.992(14)
P(1)–C(8)	1.859(14)	P(1)–C(14)	1.752(14)
O(1)–C(1)	1.150(19)	O(2)–C(2)	1.271(20)
O(3)–C(3)	1.029(18)	O(4)–C(4)	1.054(18)
C(5)–C(6)	1.542(20)	C(6)–C(7)	1.273(29)
Bond angles			
P(2)–Mo–P(1)	82.1(1)	P(2)–Mo–C(1)	90.9(5)
P(1)–Mo–C(1)	171.2(4)	P(2)–Mo–C(2)	176.8(4)
P(1)–Mo–C(2)	94.9(4)	C(1)–Mo–C(2)	92.2(6)
P(2)–Mo–C(3)	94.4(5)	P(1)–Mo–C(3)	91.7(5)
C(1)–Mo–C(3)	83.5(6)	C(2)–Mo–C(3)	86.9(6)
P(2)–Mo–C(4)	81.2(5)	P(1)–Mo–C(4)	88.0(5)
C(1)–Mo–C(4)	96.2(6)	C(2)–Mo–C(4)	97.5(6)
C(3)–Mo–C(4)	175.6(7)	Mo–P(2)–C(6)	105.2(5)
Mo–P(2)–C(20)	132.1(4)	C(6)–P(2)–C(20)	103.2(6)
Mo–P(2)–C(26)	114.5(5)	C(6)–P(2)–C(26)	107.8(6)
C(20)–P(2)–C(26)	92.0(6)	Mo–P(1)–C(5)	105.2(5)
Mo–P(1)–C(8)	116.0(5)	C(5)–P(1)–C(8)	113.3(6)
Mo–P(1)–C(14)	122.7(5)	C(5)–P(1)–C(14)	97.6(6)
C(8)–P(1)–C(14)	100.9(6)	Mo–C(1)–O(1)	177.7(10)
Mo–C(2)–O(2)	177.4(10)	Mo–C(3)–O(3)	179.0(15)
Mo–C(4)–O(4)	177.9(16)	P(1)–C(5)–C(6)	114.7(9)
P(2)–C(6)–C(5)	110.9(10)	P(2)–C(6)–C(7)	123.1(16)
C(5)–C(6)–C(7)	126.0(17)	P(2)–C(26)–C(31)	118.5(11)

Table 4
Selected bond lengths (Å) and angles (°) for **6**

Bond lengths			
Mo–C(2)#1	1.945(12)	Mo–C(2)	1.945(12)
Mo–C(1)	2.02(2)	Mo–C(3)	2.04(2)
Mo–P	2.488(2)	Mo–P#1	2.488(2)
P–C(4)	1.822(9)	P–C(10)	1.831(9)
P–C(16)	1.832(8)	O(1)–C(1)	1.13(2)
O(2)–C(2)	1.140(11)	O(3)–C(3)	1.108(14)
C(16)–C(16)#1	1.34(2)	C(16)–C(17)	1.46(2)
Bond angles			
C(2)#1–Mo–C(2)	92.3(6)	C(2)#1–Mo–C(1)	89.9(4)
C(2)–Mo–C(1)	89.9(4)	C(2)#1–Mo–C(3)	87.0(4)
C(2)–Mo–C(3)	87.0(4)	C(1)–Mo–C(3)	175.5(6)
C(2)#1–Mo–P	172.2(3)	C(2)–Mo–P	94.5(3)
C(1)–Mo–P	93.9(3)	C(3)–Mo–P	89.6(3)
C(2)#1–Mo–P#1	94.5(3)	C(2)–Mo–P#1	172.2(3)
C(1)–Mo–P#1	93.9(3)	C(3)–Mo–P#1	89.6(3)
P–Mo–P#1	78.37(11)	C(4)–P–C(10)	102.4(4)
C(4)–P–C(16)	104.3(4)	C(10)–P–C(16)	102.7(4)
C(4)–P–Mo	114.9(3)	C(10)–P–Mo	120.9(3)
C(16)–P–Mo	109.8(3)	O(1)–C(1)–Mo	177.1(14)
O(2)–C(2)–Mo	179.3(10)	O(3)–C(3)–Mo	175(2)
C(16)#1–C(16)–C(17)	116.7(7)	C(16)#1–C(16)–P	119.6(3)
C(17)–C(16)–P	123.7(8)		

is a weaker donor than the alkyl phosphine (P1). For the same reason the Mo–C2 (2.173(17) Å) bond distance is greater than the Mo–C1 (1.959(15) Å) distance. The C–O bond lengths of the two mutually *trans* carbonyls (1.029(18) and 1.054(18) Å) are less than those of the two carbonyls *trans* to the phosphorus atoms (1.150(19) and 1.271(20) Å respectively). For complex **5**, the C5–C6 carbon–carbon distance (1.542(20) Å) is greater than the C6–C7 distance (1.273(29) Å), as would be expected for a single and double bond respectively. Moreover, the angles C7–C6–C5 (126.0(17)°) and P2–C6–C7 (123.1(16)°) suggest that C6 is sp^2 hybridized. For complex **6** the molybdenum–carbon bonds for the mutually *trans* carbonyl groups, Mo–C1 (2.02(2) Å) and Mo–C3 (2.04(2) Å), are longer than those for the carbonyls *trans* to the phosphine ligands, Mo–C2#1 (1.945(12) Å)and Mo–C2 (1.945(12) Å), indicating the presence of a stronger metal–carbon bonding interaction in the latter case. This also results in an elongation of the C–O (1.140(11) Å) bond lengths of the carbonyl

Table 5
Selected bond lengths (Å) and angles (°) for **8**

Bond lengths			
Mo(1)–C(3)	1.98(2)	Mo(1)–C(1)	1.990(13)
Mo(1)–C(4)	2.010(14)	Mo(1)–C(2)	2.032(14)
Mo(1)–P(1)	2.460(4)	Mo(1)–P(2)	2.474(4)
Mo(1)–Mo(2)	3.022(4)	Mo(2)–C(6)	1.978(14)
Mo(2)–C(8)	1.99(2)	Mo(2)–C(7)	2.00(2)
Mo(2)–C(5)	2.03(2)	Mo(2)–P(1)	2.459(4)
Mo(2)–P(2)	2.467(4)	P(1)–C(9)	1.819(13)
P(1)–C(15)	1.833(12)	P(2)–C(21)	1.802(12)
P(2)–C(27)	1.827(13)	O(1)–C(1)	1.148(12)
O(2)–C(2)	1.131(12)	O(3)–C(3)	1.157(14)
O(4)–C(4)	1.128(13)	O(5)–C(5)	1.133(13)
O(6)–C(6)	1.160(13)	O(7)–C(7)	1.136(14)
O(8)–C(8)	1.15(2)		
Bond angles			
O(3)–Mo(1)–C(1)	87.8(5)	C(3)–Mo(1)–C(4)	88.1(6)
C(1)–Mo(1)–C(4)	90.4(5)	C(3)–Mo(1)–C(2)	89.0(5)
C(1)–Mo(1)–C(2)	176.6(5)	C(4)–Mo(1)–C(2)	88.1(5)
C(3)–Mo(1)–P(1)	82.8(4)	C(1)–Mo(1)–P(1)	96.7(4)
C(4)–Mo(1)–P(1)	168.3(4)	C(2)–Mo(1)–P(1)	84.3(3)
C(3)–Mo(1)–P(2)	170.2(4)	C(1)–Mo(1)–P(2)	84.6(4)
C(4)–Mo(1)–P(2)	85.7(4)	C(2)–Mo(1)–P(2)	98.4(3)
P(1)–Mo(1)–P(2)	104.25(13)	C(3)–Mo(1)–Mo(2)	134.6(4)
C(1)–Mo(1)–Mo(2)	92.0(4)	C(4)–Mo(1)–Mo(2)	137.3(4)
C(2)–Mo(1)–Mo(2)	91.3(3)	P(1)–Mo(1)–Mo(2)	52.08(9)
P(2)–Mo(1)–Mo(2)	52.19(10)	C(6)–Mo(2)–C(8)	87.9(6)
C(6)–Mo(2)–C(7)	89.0(6)	C(8)–Mo(2)–C(7)	89.3(6)
C(6)–Mo(2)–C(5)	178.6(6)	C(8)–Mo(2)–C(5)	90.9(6)
C(7)–Mo(2)–C(5)	91.6(6)	C(6)–Mo(2)–P(1)	97.0(4)
C(8)–Mo(2)–P(1)	170.2(4)	C(7)–Mo(2)–P(1)	82.3(4)
C(5)–Mo(2)–P(1)	84.3(4)	C(6)–Mo(2)–P(2)	85.0(4)
C(8)–Mo(2)–P(2)	84.3(4)	C(7)–Mo(2)–P(2)	171.4(4)
C(5)–Mo(2)–P(2)	94.2(4)	P(1)–Mo(2)–P(2)	104.51(13)
C(6)–Mo(2)–Mo(1)	90.7(4)	C(8)–Mo(2)–Mo(1)	136.6(4)
C(7)–Mo(2)–Mo(1)	134.0(4)	C(5)–Mo(2)–Mo(1)	89.8(4)
P(1)–Mo(2)–Mo(1)	52.12(10)	P(2)–Mo(2)–Mo(1)	52.40(9)
C(9)–P(1)–C(15)	100.1(6)	C(9)–P(1)–Mo(2)	123.6(5)
C(15)–P(1)–Mo(2)	118.7(4)	C(9)–P(1)–Mo(1)	116.7(4)
C(15)–P(1)–Mo(1)	122.9(5)	Mo(2)–P(1)–Mo(1)	75.80(12)
C(21)–P(2)–C(27)	100.7(6)	C(21)–P(2)–Mo(2)	119.0(4)
C(27)–P(2)–Mo(2)	121.7(4)	C(21)–P(2)–Mo(1)	124.5(5)
C(27)–P(2)–Mo(1)	116.2(4)	Mo(2)–P(2)–Mo(1)	75.41(12)
O(1)–C(1)–Mo(1)	178.9(12)	O(2)–C(2)–Mo(1)	175.9(11)
O(3)–C(3)–Mo(1)	179.5(13)	O(4)–C(4)–Mo(1)	177.7(13)
O(5)–C(5)–Mo(2)	176.3(12)	O(6)–C(6)–Mo(2)	178.9(12)
O(7)–C(7)–Mo(2)	177(2)	O(8)–C(8)–Mo(2)	179.9(14)

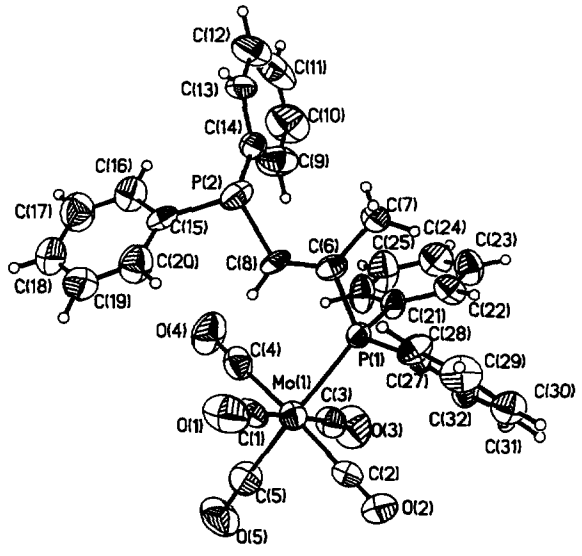

Fig. 4. Structural drawing of **9** showing the atom numbering scheme (40% probability ellipsoids). Hydrogen atoms have an arbitrary radius of 0.1 Å.

groups *trans* to the phosphorus donor atoms. The C17–C16 (1.46(2) Å) and C16–C16#1 (1.34(2) Å) distances are in accord with the presence of a single and double bond respectively. Similarly, the bond angles C17–C16–P (123.7(8)°) and C16#1–C16–P (119.6(3)°) confirm the presence of sp^2 hybridization at C16.

The molecular structure for the bridged phosphide complex **8** is shown in Fig. 3, and selected bond distances and angles are listed in Table 5. The structure is characterized by a planar geometry for the Mo_2P_2 core, similar to that found in $Mo_2(CO)_8(\mu\text{-}PEt_2)_2$ [19]. The metal–metal bond distance, 3.022(4) Å, signifies the presence of a single bond between the molybdenum atoms and is in close agreement with other reported values [19]. The metal–phosphorus bond lengths which range from 2.459(4) to 2.474(4) Å, the average values of the Mo–C (2.001(14) Å) and C–O (1.143(14) Å) bond lengths, and the Mo–C–O bond angles (178.0(14)°) are in the normal ranges [19].

The molecular structure of complex **9** is shown in Fig. 4, and selected bond angles and distances are listed in Table 6. The structure of this complex is very similar to that of complex **3**, except that in this new complex the diphosphine ligand has only one arm coordinated to the metal while the other end is free. The molybdenum–carbon bond distances for the four carbonyls *cis* to the phosphorus atom P1 (2.01(2) Å av.) are longer than that for the *trans* carbonyl (Mo1–C5 1.94(2) Å). This arises from the greater donor ability of the phosphine ligand compared with carbon monoxide. Greater backbonding into the π^* orbital of the CO ligand *trans* to the phosphine weakens the C–O bond and hence the *trans* C5–O5 (1.16(2) Å) distance is

Table 6
Selected bond lengths (Å) and angles (°) for **9**

Bond lengths			
Mo(1)–C(5)	1.94(2)	Mo(1)–C(3)	1.980(14)
Mo(1)–C(4)	2.01(2)	Mo(1)–C(2)	2.02(2)
Mo(1)–C(1)	2.02(2)	Mo(1)–P(1)	2.518(4)
P(1)–C(27)	1.813(13)	P(1)–C(21)	1.839(13)
P(1)–C(6)	1.840(11)	P(2)–C(15)	1.827(14)
P(2)–C(8)	1.834(11)	P(2)–C(9)	1.84(2)
O(1)–C(1)	1.120(14)	O(2)–C(2)	1.13(2)
O(3)–C(3)	1.130(14)	O(4)–C(4)	1.14(2)
O(5)–C(5)	1.16(2)	C(6)–C(8)	1.31(2)
C(6)–C(7)	1.53(2)		
Bond angles			
C(5)–Mo(1)–C(3)	86.7(6)	C(5)–Mo(1)–C(4)	88.8(6)
C(3)–Mo(1)–C(4)	90.3(6)	C(5)–Mo(1)–C(2)	88.5(6)
C(3)–Mo(1)–C(2)	89.2(6)	C(4)–Mo(1)–C(2)	177.3(6)
C(5)–Mo(1)–C(1)	92.1(6)	C(3)–Mo(1)–C(1)	177.0(6)
C(4)–Mo(1)–C(1)	92.3(6)	C(2)–Mo(1)–C(1)	88.1(6)
C(5)–Mo(1)–P(1)	176.4(5)	C(3)–Mo(1)–P(1)	90.0(4)
C(4)–Mo(1)–P(1)	92.4(4)	C(2)–Mo(1)–P(1)	90.2(4)
C(1)–Mo(1)–P(1)	91.2(4)	C(27)–P(1)–C(21)	106.4(6)
C(27)–P(1)–C(6)	103.4(6)	C(21)–P(1)–C(6)	98.7(5)
C(27)–P(1)–Mo(1)	111.3(4)	C(21)–P(1)–Mo(1)	114.6(4)
C(6)–P(1)–Mo(1)	120.8(5)	C(15)–P(2)–C(8)	97.9(6)
C(15)–P(2)–C(9)	101.6(7)	C(8)–P(2)–C(9)	104.2(6)
O(1)–C(1)–Mo(1)	176.9(13)	O(2)–C(2)–Mo(1)	178(2)
O(3)–C(3)–Mo(1)	177.6(14)	O(4)–C(4)–Mo(1)	178(2)
O(5)–C(5)–Mo(1)	177(2)	C(8)–C(6)–C(7)	123.3(10)
C(8)–C(6)–P(1)	118.1(10)	C(7)–C(6)–P(1)	118.4(9)
C(6)–C(8)–P(2)	125.5(10)		

greater than the other four C–O bond lengths (1.13(2) Å av.). In this *trans* diphosphine complex the C6–C8 (1.31(2) Å) and C6–C7 (1.53(2) Å) distances establish the presence of double and single bonds respectively. The angles C7–C6–C8 (123.3(10)°) and C7–C6–P1 (118.4(9)°) are close to 120°, suggesting the presence of sp^2 hybridization at C6 as expected.

3. Experimental details

3.1. Reagents and physical measurements

Commercially available, reagent grade chemicals were used unless otherwise indicated. All experiments were performed under a dry nitrogen atmosphere using standard Schlenk line techniques. $(RPh_2P)Mo(CO)_5$ (R = H, $-CH_2C{\equiv}CH$) were prepared by literature methods [12]. Tetrahydrofuran was distilled under nitrogen from sodium benzophenoneketyl, and diglyme was distilled under nitrogen from sodium. Silica gel for column chromatography (grade 12, 28–200 mesh) was obtained from Aldrich. Melting points were determined on a Mel-Temp apparatus and are uncorrected. Elemental analyses were performed by Galibraith Laboratories, Knoxville, TN. Solution infrared spectra were obtained on Perkin–Elmer 599 and Perkin–Elmer Paragon 1000 PC FT spectrometers in sealed CaF_2 cells. $^{31}P\{^1H\}$, $^{13}C\{^1H\}$ and ^1H NMR spectra were recorded at 121.66 (202.35), 75 (125.71) and 300 (499.86) MHz respectively on either a General Electric GN-300 or a Varian Unity Plus-500 spectrometer. Proton and carbon chemical shifts are relative to internal Me_4Si, phosphorus chemical shifts are relative to external PPh_3 ($\delta^{31}P = -6.0$ ppm); all shifts to low field (high frequency) are positive.

3.2. Base catalyzed reaction of 1 with 2a

(A) To a solution of 3.105 g (7.35 mmol) of **1** in freshly distilled THF was added 3.381 g (7.35 mmol) of **2a**, and the reaction mixture was stirred under nitrogen for 10 min to dissolve the contents. To this solution was added 0.5 g (4.46 mmol) of potassium tertiary-butoxide and the resultant orange mixture was refluxed gently for 24 h under nitrogen. After cooling to room temperature, 100 ml of ether and 100 ml of 1.0 M HCl were added and the contents in the reaction flask were transferred to a separatory funnel. The aqueous layer was removed and the organic phase was washed with another 2 × 100 ml of 1.0 M HCl, followed by 2 × 100 ml of water. The organic phase was dried with magnesium sulfate and filtered. The solvent was removed by rotary evaporation. The residue was dissolved in a minimum volume of dichloromethane, followed by addition of an equal volume of methanol. This mixture was then cooled to −20 °C, and after two days 1.82 g (2.06 mmol) of colorless crystals of **4** separated out. Trace amounts of another compound were also detected by $^{31}P\{^1H\}$ NMR spectroscopy (δ 65.15 and 43.87 ppm, J_{PP} = 11.8 Hz), but we were unable to separate it by fractional crystallization. The mother liquor was evaporated to dryness and the residue (3.92 g) was purified by column chromatography on silica gel using a solution of 5% benzene in hexane as the eluant. The polarity of the solution was gradually increased. 20 fractions of 50–70 ml by volume were collected and monitored by TLC and $^{31}P\{^1H\}$ NMR spectroscopy. From the first five fractions about 0.58 g of unreacted starting material (mainly **2c**) was retrieved with trace amounts of oxides. Fractions 6–12 gave 0.95 g (1.08 mmol) of **3** with trace amounts of another compound as an impurity in the later fractions, which could not be separated for complete characterization. The polarity of the solvent was then changed to 10% benzene in hexane. Complex **4** was eluted next in fractions 13–14 and 0.2 g (0.23 mmol) was recovered. Fraction 14 was contaminated with the same impurities in trace amounts as found in the first batch of crystals of **4**. The column was then eluted with 15% benzene in hexane solution. Fractions 15–16 contained trace amounts of **4** which could not be recovered. The polarity of the eluant was then changed to 20% benzene in hexane and subsequently gradually increased to around 75% benzene in hexane. Complex **5** (1.82 g, 2.9 mmol) was eluted last from the column in fractions 17–20. All the above mentioned complexes were recrystallized from a 1:1 mixture of dichloromethane and methanol.

(B) Potassium tertiary butoxide 0.25 g (2.23 mmol) was added to a solution containing 4.295 g (10.2 mmol) of **1** and 4.68 g (10.2 mmol) of **2a** in 250 ml of freshly distilled diglyme. The resultant yellow–orange solution was refluxed for 24 h with stirring under nitrogen. The contents of the reaction flask were cooled to room temperature and the solvent was removed by vacuum distillation. The residue was dissolved in 150 ml of ether and 50 ml hexane and then transferred into a 500 ml separatory funnel. The organic layer was washed with 3 × 100 ml portions of 1.0 M HCl and then 3 × 100 ml portions of water followed by drying with $MgSO_4$. The solvent was removed by rotary evaporation. This crude product was purified by column chromatography on silica gel with 5% benzene in hexane solution as the eluant. 35 fractions in volumes of 50–75 ml each were collected and monitored by TLC and $^{31}P\{^1H\}$ NMR spectroscopy. Approximately 0.05 g of oxides and unreacted starting materials (mainly **2c**) from fractions 1–8 and 2.4 g (2.72 mmol) of **3** were recovered from fractions 9–21. The later fractions of this batch (18–21) contained at least two other compounds in minor quantities with the same r_f value and could not be separated for characterization. The polarity

of the eluant was then increased to 10% benzene in hexane. This gave about 0.05 g of **3** with considerable amounts of the aforementioned unidentified compounds from fractions 22–24. The benzene concentration of the eluant was increased to almost 50%, as fractions 25–26 contained no dissolved materials. When fraction 27 was collected and left at −20 °C for 5 h, 0.30 g (0.39 mmol) of flaky white crystals of **7** crystallized out. The mother liquor of this fraction and fractions 28–32 (eluted with 3:1 benzene:hexane) gave 2.93 g (4.74 mmol) of **5**. Trace amounts of **8** which were present in some of the above fractions were isolated by concentrating the fractions followed by centrifugation, whereby **8** settled down as a red precipitate. The supernate was decanted and left at −20 °C for crystals of **5** to precipitate. Fractions 33–35 obtained by eluting with pure benzene gave 0.45 g (0.57 mmol) of **8**. The complexes obtained from this separation were recrystallized from a 1:1 mixture of dichloromethane and methanol.

3.3. Base catalyzed reaction of *4*

To a solution of 0.10 g (0.122 mmol) of **4** in 100 ml of freshly distilled diglyme was added 0.052 g (0.46 mmol) of potassium tertiary butoxide and the reaction mixture was refluxed for 24 h with stirring under an atmosphere of nitrogen. The contents of the flask were cooled and the solvent was removed by vacuum distillation. The residue was dissolved in 50 ml ether and 50 ml hexane. The resultant mixture was then transferred into a separatory funnel and the organic layer was washed with 2 × 100 ml portions of 1.0 M HCl solution followed by 2 × 100 ml portions of distilled water. The organic phase was then dried with magnesium sulfate and the solvents were removed by rotary evaporation. The residue was dissolved in a minimum volume of dichloromethane and filtered. To the filtrate was added an equal volume of ether and methanol. It was allowed to stand for 24 h at −20 °C, whereby 0.025 g (0.041 mmol) of pale yellow crystals of compound **6** separated out. The crystals were isolated by filtration. Removal of the solvent from the mother liquor by rotary evaporation left behind an amorphous pale white solid. The white solid was crystallized from a 1:1 mixture of dichloromethane and methanol to give 0.039 g (0.063 mmol) of colorless crystals of **5**.

3.4. Base catalyzed reaction of diphenyl phosphine with *2c*

To a solution of 1.926 g (4.186 mmol) of **2c** in 100 ml of freshly distilled diglyme was added 0.856 g (4.597 mmol) of diphenylphosphine by means of a syringe under nitrogen, and the mixture was stirred for 3–4 min. A catalytic amount of potassium tertiary butoxide was added to this reaction mixture and it was allowed to reflux for 0.75 h under an atmosphere of nitrogen with stirring. The color of the solution turned reddish brown. The contents of the reaction flask were allowed to cool and then the solvent and unreacted Ph_2PH were removed by vacuum distillation. The residue was washed with 20 ml cold hexane and then dissolved in a minimum volume of dichloromethane and filtered through a 1 cm thick Celite bed. To the filtrate obtained was added an equal volume of methanol and the mixture was allowed to crystallize at −20 °C. Pale yellow crystals of complex **6** (1.89 g, 3.06 mmol) separated out after 24 h.

3.5. Characterization of complexes *3–8*

3. Colorless solid. M.p. 148 °C (decomp.). IR (CH_2Cl_2): $\nu_{CO}(cm^{-1})$ 2073 (m), 2064 (sh), 1990 (sh), 1950 (s), 1938 (sh). $^{31}P\{^1H\}$ NMR ($CDCl_3$, 202.35 MHz) δ 22.2 (d, $^3J_{PP}$ = 26.9 Hz, P_A), 53.0 (d, $^3J_{PP}$ = 26.9 Hz, P_x). ^1H NMR ($CDCl_3$, 500 MHz) δ 1.59 (dd, $^3J_{PH}$ = 10.5 Hz, $^4J_{HH}$ = 0.5 Hz, 3H, CH_3), 7.31 (ddq, $^3J_{PH}$ = 20.99 Hz, $^2J_{PH}$ = 14.49 Hz, $^4J_{HH}$ = 0.5 Hz, 1H, C=C*H*), 7.36–7.54 (m, 20H, aromatic H's). $^{13}C\{^1H\}$ NMR ($CDCl_3$, 125.71 MHz) δ 19.43 (dd, $^2J_{PC}$ = 10.56 Hz, $^3J_{PC}$ = 9.37 Hz, C_α), 128.80 (d, $^3J_{PC}$ = 6.66 Hz, C_m), 128.87 (d, $^3J_{PC}$ = 7.17 Hz, C_m), 130.18 (d, $^4J_{PC}$ = 1.89 Hz, C_p), 130.40 (d, $^4J_{PC}$ = 1.76 Hz, C_p), 132.10 (d, $^2J_{PC}$ = 12.45 Hz, C_o), 132.62 (d, $^2J_{PC}$ = 11.94 Hz, C_o), 133.67 (d, $^1J_{PC}$ = 34.32 Hz, C_i), 135.97 (d, $^1J_{PC}$ = 37.71 Hz, C_i), 141.47 (dd, $^1J_{PC}$ = 22.5 Hz, $^2J_{PC}$ = 15.58 Hz, C_γ), 148.17 (dd, $^1J_{PC}$ = 19.36 Hz, $^2J_{PC}$ = 2.14 Hz, C_β), 205.16 (d, $^2J_{PC}$ = 8.42 Hz, $4CO_{a/a'}$), 205.40 (d, $^2J_{PC}$ = 8.67 Hz, $4CO_{a/a'}$), 209.72 (d, $^2J_{PC}$ = 22.38 Hz, $CO_{b/b'}$), 209.73 (d, $^2J_{PC}$ = 23.51 Hz, $CO_{b/b'}$). Anal. Found: C, 50.18; H, 2.59. $C_{37}H_{24}Mo_2O_{10}P_2$ Calc.: C, 50.36; H, 2.74%.

4. Colorless solid. M.p. 175 °C (decomp.). IR (CH_2Cl_2): $\nu_{CO}(cm^{-1})$ 2073 (m), 2064 (sh), 1990 (sh), 1949 (s), 1938 (sh). $^{31}P\{^1H\}$ NMR ($CDCl_3$, 121.66 MHz) δ 22.5 (d, $^3J_{PP}$ = 15.3 Hz, P_A), 47.3 (d, $^3J_{PP}$ = 15.3 Hz, P_x). ^1H NMR ($CDCl_3$, 300 MHz) δ 3.15 (dd, $^3J_{PH}$ = 6.30 Hz, $^2J_{PH}$ = 4.80 Hz, 2H, C*H*$_2$), 6.01 (d, $^3J_{PH_a}$ = 40.0 Hz, 1H, H_a), 6.08 (d, $^3J_{PH_b}$ = 19.0 Hz, 1H, H_b), 7.18–7.54 (m, 20H, aromatic H's). $^{13}C\{^1H\}$ NMR ($CDCl_3$, 125.71 MHz) δ 35.14 (dd, $^1J_{PC}$ = 15.28 Hz, $^2J_{PC}$ = 9.36 Hz, C_γ), 128.74 (d, $^3J_{PC}$ = 9.3 Hz, C_m), 128.87 (d, $^3J_{PC}$ = 9.05 Hz, C_m), 130.14 (d, $^4J_{PC}$ = 1.89 Hz, C_p), 130.45 (d, $^4J_{PC}$ = 1.77 Hz, C_p), 131.39 (d, $^2J_{PC}$ = 11.82 Hz, C_o), 132.48 (d, $^2J_{PC}$ = 12.07 Hz, C_o), 133.38 (d, $^1J_{PC}$ = 34.19 Hz, C_i), 135.49 (d, $^3J_{PC}$ = 34.07 Hz, C_α), 135.98 (d, $^1J_{PC}$ = 37.46 Hz, C_i), 135.66 (dd, $^1J_{PC}$ = 21.37 Hz, $^2J_{PC}$ = 3.21 Hz, C_β), 205.24 (d, $^2J_{PC}$ = 8.67 Hz, $4CO_{a/a'}$), 205.36 (d, $^2J_{PC}$ = 8.67 Hz, $4CO_{a/a'}$), 209.64 (d, $^2J_{PC}$ = 21.37 Hz, $CO_{b/b'}$), 209.82 (d, $^2J_{PC}$ = 21.62 Hz, $CO_{b/b'}$). Anal. Found: C, 50.22; H, 2.81. $C_{37}H_{24}Mo_2O_{10}P_2$ Calc.: C, 50.36; H, 2.74%.

5. Colorless solid. M.p. 168 °C (decomp.). IR (CH_2Cl_2): $\nu_{CO}(cm^{-1})$ 2022 (m), 1911 (s), 1886 (sh). $^{31}P\{^1H\}$ NMR ($CDCl_3$, 121.66 MHz) δ 36.9 (d, $^2J_{PP}$ = 7.5 Hz, P_A), δ 53.9 (d, $^2J_{PP}$ = 7.5 Hz, P_x). ^1H NMR ($CDCl_3$, 300 MHz) δ 3.29 (dd, $^2J_{PH}$ = 18.61 Hz, $^3J_{PH}$ = 10.21 Hz, 2H, CH_2), 5.14 (dd, $^3J_{PH_b}$ = 11.71 Hz, $^2J_{H_aH_b}$ = 3.61 Hz, 1H, H_b), 5.96 (dd, $^3J_{PH_a}$ = 23.71 Hz, $^2J_{H_aH_b}$ = 3.61 Hz, 1H, H_a), 7.33–7.62 (m, 20H, aromatic H's). $^{13}C\{^1H\}$ NMR ($CDCl_3$, 75 MHz) δ 39.64 (dd, $^1J_{PC}$ = 31.93 Hz, $^2J_{PC}$ = 22.41 Hz, C_γ), 126.02 (d, $^2J_{PC}$ = 12.55 Hz, C_α), 128.52 (d, $^3J_{PC}$ = 9.07 Hz, C_m), 128.58 (d, $^3J_{PC}$ = 9.60 Hz, C_m), 129.81 (s, C_p), 130.10 (s, C_p), 131.58 (d, $^2J_{PC}$ = 12.24 Hz, C_o), 132.92 (d, $^2J_{PC}$ = 13.15 Hz, C_o), 133.58 (d, $^1J_{PC}$ = 35.07 Hz, C_i), 136.76 (d, $^1J_{PC}$ = 32.80 Hz, C_i), 144.82 (dd, $^1J_{PC}$ = 28.57 Hz, $^2J_{PC}$ = 13.07 Hz, C_β), 209.57 (apparent t, $^2J_{PC}$ = 8.77 Hz, $CO_{a,a'}$), 216.68 (dd, $^2J_{PC}$ = 24.58 Hz, $^2J_{PC}$ = 8.98 Hz, $CO_{b\ or\ b'}$), 217.01 (dd, $^2J_{PC}$ = 24.48 Hz, $^2J_{PC}$ = 8.92 Hz, $CO_{b\ or\ b'}$). Anal. Found: C, 60.28; H, 3.73. $C_{31}H_{24}MoO_4P_2$ Calc.: C, 60.21; H, 3.91%.

6. Pale yellow solid. M.p. 175 °C (decomp.). IR (CH_2Cl_2): $\nu_{CO}(cm^{-1})$ 2024 (m), 2012 (sh), 1924 (sh), 1908 (s), 1890 (sh). $^{31}P\{^1H\}$ NMR ($CDCl_3$, 121.66 MHz) δ 52.1 (d, $^2J_{PP}$ = 6.3 Hz, P_A), 70.1 (d, $^2J_{PP}$ = 6.3 Hz, P_x). ^1H NMR ($CDCl_3$, 500 MHz) δ 2.17 (dd, $^3J_{PH}$ = 6 Hz, $^4J_{HH}$ = 1 Hz, 3H, CH_3), 7.35–7.60 (m, 21H, H_γ and aromatic H's). $^{13}C\{^1H\}$ NMR ($CDCl_3$, 125.71 MHz) δ 20.40 (dd, $^2J_{PC}$ = 1.07 Hz, $^3J_{PC}$ = 15.78 Hz, C_α), 128.54 (d, $^3J_{PC}$ = 8.79 Hz, C_m), 128.59 (d, $^3J_{PC}$ = 9.18 Hz, C_m), 129.75 (s, C_p), 129.76 (s, C_p), 131.59 (d, $^2J_{PC}$ = 12.82 Hz, C_o), 131.98 (d, $^2J_{PC}$ = 13.15 Hz, C_o), 134.91 (dd, $^1J_{PC}$ = 33.69 Hz, $^4J_{PC}$ = 2.26 Hz, C_i), 137.18 (dd, $^1J_{PC}$ = 33.65 Hz, $^4J_{PC}$ = 1.70 Hz, C_i), 144.82 (apparent t, $^1J_{PC}$ = $^2J_{PC}$ = 38.3 Hz, C_γ), 157.16 (dd, $^1J_{PC}$ = 30.17 Hz, $^2J_{PC}$ = 23.88 Hz, C_β), 208.98 (apparent t, $^2J_{PC}$ = 8.55 Hz, $CO_{a,a'}$), 216.78 (dd, $^2J_{PC}$ = 20.08 Hz, $^2J_{PC}$ = 8.24 Hz, $CO_{b\ or\ b'}$), 217.67 (dd, $^2J_{PC}$ = 26.09 Hz, $^2J_{PC}$ = 8.61 Hz, $CO_{b\ or\ b'}$). Anal. Found: C, 60.06; H, 4.12. $C_{31}H_{24}MoO_4P_2$ Calc.: C, 60.21; H, 3.91%.

7. Flaky white solid. M.p. 238–240 °C (decomp.). IR (CH_2Cl_2): $\nu_{CO}(cm^{-1})$ 1938 (s), 1842 (br). $^{31}P\{^1H\}$ NMR ($CDCl_3$, 202.35 MHz) δ 47.0 (d, $^2J_{PP}$ = 1.5 Hz, P_A, $P_{A'}$), 82.9 (apparent t, $^2J_{PP}$ = 1.5 Hz, P_x). ^1H NMR ($CDCl_3$, 500 MHz) δ 2.56 (m, 4H, 2CH_2), 4.01 (apparent td, $^2J_{PH}$ = 9.83 Hz, $^3J_{PH}$ = 35.0 Hz, 1H, CH), 6.84–7.74 (m, 30H, aromatic H's). $^{13}C\{^1H\}$ NMR ($CDCl_3$, 125.71 MHz) δ 30.58 (m, C_α), 38.32 (dt, $^1J_{PC}$ = 24.39 Hz, $^2J_{PC}$ = 17.22 Hz, C_β), 127.64 (T, $|^3J_{PC} + {}^5J_{PC}|$ = 9.43 Hz, C_m), 127.91 (T, $|^3J_{PC} + {}^5J_{PC}|$ = 9.05 Hz, C_m), 128.18 (s, C_p), 128.41 (d, $^3J_{PC}$ = 8.92 Hz, C_m), 128.44 (s, C_p), 129.81 (d, $^4J_{PC}$ = 1.63 Hz, C_p), 130.58 (T, $|^2J_{PC} + {}^4J_{PC}|$ = 13.32 Hz, C_o), 131.33 (T, $|^2J_{PC} + {}^4J_{PC}|$ = 12.57 Hz, C_o), 132.61 (d, $^2J_{PC}$ = 13.07 Hz, C_o), 134.72 (dt, $^1J_{PC}$ = 27.28 Hz, $^3J_{PC}$ = 2.64 Hz, C_i), 136.70 (m, C_i), 139.76 (T, $|^1J_{PC} + {}^3J_{PC}|$ = 36.83 Hz, C_i), 222.38 (apparent q, $^2J_{PC}$ = 8.25 Hz, $CO_{a,b,c}$). Anal. Found: C, 64.82; H, 4.39. $C_{42}H_{35}MoO_3P_3$ Calc.: C, 64.96; H, 4.54%.

8. Red solid. M.p. 145 °C (decomp.). IR (CH_2Cl_2): $\nu_{CO}(cm^{-1})$ 2033 (m), 1996 (w, sh), 1967 (s). $^{31}P\{^1H\}$ NMR ($CDCl_3$, 121.66 MHz) δ 231.7 (s, 2P). ^1H NMR ($CDCl_3$, 500 MHz) δ 7.32–7.78 (m, 20H, aromatic H's). $^{13}C\{^1H\}$ NMR ($CDCl_3$, 125.71 MHz) δ 128.34 (T, $|^3J_{PC} + {}^5J_{PC}|$ = 9.30 Hz, C_m), 129.70 (s, C_p), 132.80 (T, $|^2J_{PC} + {}^4J_{PC}|$ = 9.68 Hz, C_o), 141.26 ([AXX'], 6 line, [20] $^1J_{PC}$ = 35.29 Hz, $^2J_{PP}$ = 14.03 Hz, $^3J_{PC}$ = 1.35 Hz, C_i), 199.86 (t, $^2J_{PC}$ = 5.22 Hz, 4CO_a), 214.49 (T, $|^2J_{PC} + {}^2J_{P'C}|$ = 43.1 Hz, 4CO_b). Anal. Found: C, 48.63; H, 2.61. $C_{32}H_{20}Mo_2O_8P_2$ Calc.: C, 48.88; H, 2.56%.

3.6. X-ray data collection and processing

Crystals of **3**, **4**, **5**, **6**, **8** and **9** were isolated from CH_2Cl_2/CH_3OH at −20 °C. Suitable crystals were mounted on glass fibers and placed on a Siemens P4 diffractometer. Crystal data and details of collection are given in Table 7. Intensity data were taken in the ω-mode at 298 K with Mo Kα graphite monochromated radiation (λ = 0.71073 Å). Two check reflections, monitored every 100 reflections, showed random (< 2%) variation during the data collections. Unit cell parameters were determined by least-squares refinement of 25 reflections with 10.0° < θ < 25°. 5959 (2θ < 45°), 6416 (2θ < 45°), 4653 (2θ < 45°), 1934 (2θ < 45°), 3925 (2θ < 40°) and 4024 (2θ < 45°) reflections were measured respectively. The data were corrected for Lorentz and polarization effects and merged to give 4992 (R_f = 0.0430) with 4338 having $I > 2\sigma(I)$ regarded as observed for **3**, 5007 (R_f = 0.0930) with 4334 having $I > 2\sigma(I)$ regarded as observed for **4**, 3733 (R_f = 2.03%) with 1958 having $F > 4\sigma(I)$ regarded as observed for **5**, 2958 (R_f = 0.0595) with 2958 having $I > 2\sigma(I)$ regarded as observed for **8** and 4024 with 3355 having $I > 2\sigma(I)$ regarded as observed for **9**. All 1934 reflections for **6** were used in refinement on F^2. The data were corrected for absorption using a semi-empirical model [maximum and minimum transmission factors 0.47 (0.43), 0.84 (0.73), 0.97 (0.95), 0.95 (0.87) for **3**, **4**, **5** and **8** respectively]. For **6** XABS2 [21] was used and for **9** no absorption correction was applied. Scattering factors and corrections for anomalous dispersion were taken from a standard source [22]. Calculations were performed with the Siemens SHELXTL PLUS Vers. 5.0 software package on a personal computer. The structures were solved by direct methods. Anisotropic thermal parameters were assigned to all non-hydrogen atoms except for the phenyl ring carbons of **3** and **5**. Hydrogen atoms were refined at calculated positions with a riding model in which the C–H vector was fixed at 0.96 Å. Further details of the crystal structure investigations are available from either V.J. Catalano or J.H. Nelson.

Table 7
Crystallographic data for complexes **3**, **4**, **5**, **6**, **8** and **9**

	3	**4**	**5**	**6**	**8**	**9**
Chemical formula	$C_{37}H_{24}Mo_2O_{10}P_2$	$C_{37}H_{24}Mo_2O_{10}P_2$	$C_{31}H_{24}MoO_4P_2$	$C_{20.67}H_{15.33}Mo_{0.67}O_{2.67}P_{1.33}$	$C_{32}H_{20}Mo_2O_8P_2$	$C_{32}H_{24}MoO_5P_2$
Formula weight	882.38	882.38	618.42	411.58	786.30	646.39
Crystal system	triclinic	monoclinic	orthorhombic	orthorhombic	monoclinic	triclinic
Space group	$P\bar{1}$	$P2_1/c$	*Pbca*	*Pnma*	$P2_1/c$	$P\bar{1}$
a (Å)	10.665(1)	9.656(2)	15.049(3)	17.052(2)	9.772(3)	11.460(2)
b (Å)	12.675(2)	23.597(2)	16.822(3)	21.496(2)	19.734(6)	11.830(2)
c (Å)	14.310(2)	16.811(2)	22.356(3)	7.806(1)	16.93(3)	13.167(2)
α (°)	90.45(1)	90	90	90	90	79.50(2)
β (°)	91.12(1)	90.89(1)	90	90	103.72(9)	64.57(2)
γ (°)	96.32(1)	90	90	90	90	74.61(2)
V (Å^3)	1922.2(4)	3830.0(10)	5705.0(15)	2861.3(6)	3172(5)	1549.5(4)
Z	2	4	8	6	4	2
ρ_{calc} (g cm^{-3})	1.525	1.530	1.440	1.433	1.647	1.385
μ (cm^{-1})	7.89	7.92	6.06	6.04	9.41	5.63
$R_1(F)$ [a]	0.0618	0.0616	0.0707	0.0666	0.0557	0.0825
$wR_2(F^2)$ [b]	0.1346	0.1354	0.0758	0.1181	0.0811	0.1610

[a] $R_1(F) = \Sigma||F_o| - |F_c||/\Sigma|F_o|$.
[b] $wR_2(F^2) = [\Sigma[w(F_o^2 - F_c^2)^2]/\Sigma[w(F_o^2)^2]]^{0.5}$.

Acknowledgements

We are grateful to the donors of the Petroleum Research Fund, administered by the American Chemical Society, for financial support.

References

[1] P.M. Treichel and W.K. Wong, *Inorg. Chim. Acta, 33* (1979) 171–175; R.L. Keiter, S.L. Kaiser, N.P. Hansen, J.W. Brodack and L.W. Cary, *Inorg. Chem., 20* (1981) 283–285; R.L. Keiter, J.W. Brodack, R.D. Borger and L.W. Cary, *Inorg. Chem., 21* (1982) 1256–1259; B.N. Diel, R.C. Haltiwanger and A.D. Norman, *J. Am. Chem. Soc., 104* (1982) 4700–4701; R.L. Keiter, R.D. Borger, M.J. Madigan, S.L. Kaiser and D.L. Rowley, *Inorg. Chim. Acta, 76* (1983) L5–L6; R.L. Keiter, A.L. Rheingold, J.J. Hamerski and C.K. Castle, *Organometallics, 2* (1983) 1635–1639; J.A. Iggo and B.L. Shaw, *J. Chem. Soc., Dalton Trans.*, (1985) 1009–1013; J.A. Rahn, A. DeCian and J.H. Nelson, *Inorg. Chem., 28* (1989) 215–217; E.W. Abel, F.G.A. Stone and G. Wilkinson (eds.), *Comprehensive Organometallic Chemistry*, Pergamon Press, Oxford, 1982 and references cited therein.

[2] J.L. Bookham and W. McFarlane, *J. Chem. Soc., Dalton Trans.*, (1990) 489–494.

[3] J.L. Bookham, W. Clegg, W. McFarlane and E.S. Raper, *J. Chem. Soc., Dalton Trans.*, (1993) 3567–3573.

[4] I.J. Colquhoun, W. McFarlane and R.L. Keiter, *J. Chem. Soc., Dalton Trans.*, (1984) 455–458.

[5] R.B. King and P.N. Kapoor, *J. Am. Chem. Soc., 91* (1969) 5191–5192.

[6] A.J. Carty, D.K. Johnson and S.E. Jacobson, *J. Am. Chem. Soc., 101* (1979) 5612–5619.

[7] A.J. Carty, S.E. Jacobson, R.T. Simpson and N.J. Taylor, *J. Am. Chem. Soc., 97* (1975) 7254–7262.

[8] N.J. Taylor, S.E. Jacobson and A.J. Carty, *Inorg. Chem., 14* (1975) 2648–2653.

[9] R.T. Simpson, S.E. Jacobson, A.J. Carty, M. Mathew and G.J. Palenik, *J. Chem. Soc., Chem. Commun.*, (1973) 388–389; T. Rukachaisirikul, S. Arabi, F. Hartstock, N.C. Taylor and A.J. Carty, *Organometallics, 3* (1984) 1587–1589; A.J. Carty, N.J. Taylor and D.K. Johnson, *J. Am. Chem. Soc., 101* (1979) 5422–5424.

[10] H.B. Kagan and T.P. Dang, *J. Am. Chem. Soc., 94* (1972) 6429–6433; K. Achiwa, *J. Am. Chem. Soc., 98* (1976) 8265–8266; M.E. Wilson, R.G. Nuzzo and G.M. Whitesides, *J. Am. Chem. Soc., 100* (1978) 2269–2270; P.M. Treichel, W.L. Wong and J.C. Calabrese, *J. Organomet. Chem., 159* (1978) C20–C24; S. Brunie, J. Mazan, N. Langlois and H.B. Kagan, *J. Organomet. Chem., 114* (1976) 225–232; J.M. Brown and P.A. Chaloner, *J. Chem. Soc., Chem. Commun.*, (1978) 321–322; A.R. Sanger and K.G. Tan, *Inorg. Chim. Acta, 31* (1978) L439–L440; H. Brunner and W. Zettlmeier (eds.), *Handbook Of Enantioselective Catalysis*, Vol. II, VCH, Weinheim, 1993.

[11] W.L. Wilson, N.W. Alcock, E.C. Alyea, S. Song and J.H. Nelson, *Bull. Soc. Chim. Fr., 130* (1993) 673–682.

[12] K. Maitra, W.L. Wilson, M.M. Jemin, C. Yeung, W.S. Rader, K.D. Redwine, D.P. Striplin, V.J. Catalano and J.H. Nelson, *Synth. React. Inorg. Metall. Org. Chem., 26* (1996) 967–996.

[13] B.L. Shaw and J.P. Vessey, *J. Chem. Soc., Dalton Trans.*, (1992) 1929–1938; B.L. Shaw and J.D. Vessey, *J. Chem. Soc., Dalton Trans.*, (1991) 3303–3310.

[14] L. Horner, I. Ertel, H.D. Ruprecht and O. Belovsky, *Chem. Ber., 103* (1970) 1582–1588.

[15] W. Hewertson, I.C. Taylor and S. Triplett, *J. Chem. Soc. (C)*, (1970) 1835–1839.

[16] A.L. Crumbliss and R.J. Topping, in J.G. Verkade and L.D. Quin (eds.), *Phosphorus-31 NMR Spectroscopy in Stereochemical Analysis*, VCH, Deerfield Beach, FL, 1987, pp. 531–557.

[17] S.-G. Shyu, M. Calligaris, G. Nardin and A. Wojcicki, *J. Am. Chem. Soc., 109* (1987) 3617–3625.

[18] R.L. Keiter, E.A. Keiter, D.M. Olson, J.R. Bush, W. Lin and J.W. Berson, *Organometallics, 13* (1994) 3752–3754.

[19] M.H. Linck and L.R. Nassimbeni, *Inorg. Nucl. Chem. Lett., 9* (1973) 1105–1113.

[20] D.A. Redfield and J.H. Nelson, *Inorg. Nucl. Chem. Lett., 10* (1974) 727–733; A.W. Verstuyft, L.W. Cary and J.H. Nelson, *Inorg. Chem., 14* (1975) 1495–1501; D.A. Redfield, L.W. Cary and J.H. Nelson, *Inorg. Chem., 14* (1975) 50–59; *15* (1976) 732–734, 1128–1133.

[21] A.L. Balch, L.A. Fossett, R.G. Guimerans, M.M. Olmstead and P.E. Reedy, Jr., *Inorg. Chem., 25* (1986) 1397–1404.

[22] *International Tables For X-Ray Crystallography*, Vol. C, Reidel, Boston, 1992.